IEEE Access
Multidisciplinary | Rapid Review | Open Access Journal

Received July 1, 2018, accepted August 5, 2018, date of publication August 8, 2018, date of current version August 28, 2018.

Digital Object Identifier 10.1109/ACCESS.2018.2864347

Radar Signal Intra-Pulse Modulation Recognition Based on Convolutional Neural Network

ZHIYU QU, XIAOJIE MAO, AND ZHIAN DENG
College of Information and Telecommunication, Harbin Engineering University, Harbin 150001,China

Corresponding author: Zhian Deng (dengzhian@hrbeu.edu.cn)

This work was supported in part by the National Natural Science Foundation of China under Grant 61671168, in part by the Fundamental Research Funds for the Central Universities under Grant HEUCFJ180801 and Grant HEUCF180801, and in part by the Natural Science Foundation of Heilongjiang Province under Grant QC2016085.

ABSTRACT In this paper, to solve the problem of the low recognition rate of the existing approaches at low signal-to-noise ratio (SNR), an intra-pulse modulation recognition approach for radar signal is proposed. The approach identifies the modulation of radar signals using the techniques of time-frequency analysis, image processing, and convolutional neural network (CNN). Through Cohen class time-frequency distribution (CTFD), the time-frequency images (TFIs) of received signals are extracted. In order to obtain the high-quality TFIs of received signals, we introduce a new kernel function for the CTFD, which has stronger anti-noise ability than Choi–Williams time-frequency distribution. A series of image processing techniques, including 2-D Wiener filtering, bilinear interpolation, and Otsu method, are applied to remove the background noise of the TFI and obtain a fixed-size binary image that contains only morphological features of the TFI. We design a CNN classifier to identify the processed TFIs. The proposed approach can identify up to 12 kinds of modulation signals, including frequency modulation, phase modulation, and composite modulation. Simulation results show that, for 12 kinds of modulation signals, the proposed approach achieves an overall probability of successful recognition of 96.1% when SNR is −6 dB.

INDEX TERMS Radar signal recognition, Cohen class time frequency distribution, convolutional neural network.

I. INTRODUCTION

Radar signal intra-pulse modulation recognition is a crucial technology in radar electronic warfare (EW). It plays an important role in modern electronic support measure (ESM) system, electronic intelligence (ELINT) system and radar warning receiver [1]–[3]. The accurate recognition of intra-pulse modulation of the radar signals can help to estimate the function of radar emitters while improving the accuracy of radar signal parameter estimation. However, the pulse compression technique used in radar greatly reduces the power spectral density of radar signal. The interception and identification of radar signals have become more and more difficult. The signal-to-noise ratio (SNR) for the normal working environment of radar is also getting lower and lower. This requires that the intra-pulse modulation recognition method of radar signals has a good performance at low SNR. Furthermore, with the rapid development of radar technology, the intra-pulse modulation of radar signals are becoming more and more diversified [4]. An extensive modulation types of radar signals are also required to be recognized [5], [6]. Therefore, how to accurately recognize extensive modulation types of radar signals in low SNR environment is urgent to be solved.

The intra-pulse modulation recognition approaches of radar signals can be divided into two categories, including decision theory based approach [7], [8] and statistical pattern recognition based approach [9]–[12]. The former approach is based on probability theory and Bayesian estimation theory, which relies on the prior information of radar signals, such as probability model or some other parameters of the signals. For practical uses, the latter approach is more popular, since it performs better than the former one for the blind recognition of radar signals. The latter approach requires no prior information of radar signals. The statistical pattern recognition based approach includes two major steps: feature extraction and classification. The feature extraction uses techniques such as spectrum autocorrelation, time-frequency analysis, high-order cumulants and various transform domain analysis, etc.

The researchers have made great efforts to improve the performance of the approach based on statistical pattern recognition in low SNR environment. In [13], the

Rihaczek distribution (RD) and the Hough transform (HT) are used to concentrate the energy in time-frequency plane and extract the ratio of the minimum to the maximum of the HT and the peak number of the HT of the real part of the RD. This approach can recognize linear frequency modulation (LFM), frequency shift keying (FSK), binary phase shift keying (BPSK) and mono-pulse (MP) signals and its probability of successful recognition (PSR) can reach 90% when the SNR is above −4 dB. This approach has a strong anti-noise ability, but the identified type number of radar signals is limited. In [14] and [15], radar signals are transformed into the time-frequency domain using Choi-Williams distribution (CWD). Then, the characteristics of the signal time-frequency domain are extracted, including high-order cumulants, instantaneous frequency and all order moments, etc. These characteristics are formed as an input feature vector of the final classifier consisting of two of back-propagation (BP) neural networks. This approach can identify LFM, BPSK, Costas, Frank, P1, P2, P3, P4 signals. The overall PSR is 94.7% when the SNR is −2 dB. However, it can not identify the nonlinear frequency modulation signals and composite modulation signals. In addition, the performance of these approaches depends very much on the extracted features. These extracted features often rely on the experience of the researchers, and it is not necessarily optimal. So researchers are trying to find a way that can extract features automatically and optimally.

Recently, some researchers introduce deep learning to the field of radar signal modulation recognition, since deep learning can automatically extract the characteristics of signals and it has made great success in many fields, such as image recognition, speech recognition, object detection and so on [16]–[18]. Some approaches for radar signal modulation recognition based on deep learning have been proposed [19]–[22]. In [20], a deep neural network model based on multiple restricted Boltzmann machines is designed for radar signal recognition. It can identify eight kinds of radar signals (CW, PSK, DPSK, FSK, MP, LFM and NLFM) in the time domain. In [22], the convolutional neural network (CNN) based on LeNet-5 is introduced to identify the time-frequency images (TFIs) of radar signals. This approach can identify eight kinds of radar signals (BPSK, LFM, Costas, Frank and T1-T4) when SNR is above −2 dB. However, there are still many problems with these approaches. First, the modulation type of the recognizable signal is limited in low SNR environment. Second, if the test samples and training samples parameters vary greatly, the performances of these approaches will be greatly reduced, so the adaptabilities of these approaches are poor and they cannot identify radar signals with large variation range parameters.

In this paper, we propose a novel approach for radar signal intra-pulse modulation recognition which uses the techniques of time-frequency analysis, image processing and CNN based on LeNet-5. The approach can identify twelve kinds of modulation signals, including LFM, Sinusoidal frequency modulation (SFM), 2FSK, 4FSK, dual frequency modulation (DLFM), even quadratic frequency modulation (EQFM), multiple linear frequency modulation (MLFM), BPSK, Frank, MP and composite modulation (LFM-BPSK, 2FSK-BPSK). We introduce a new kernel function for Cohen class time-frequency distribution (CTFD) to extract the TFIs of radar signals. The CTFD with the new kernel function has better anti-noise ability than CWD for the proposed approach. Through a series of methods, including 2-D Wiener filtering, bilinear interpolation and Otsu method, we remove the background noise of the TFI while enhancing the robustness of the approach and a fixed-size binary image that contains only morphological features of the TFI is obtained. In addition, in order to improve the classification performance of the CNN based on LeNet-5, we increase the number of CNN layers and reset the parameters of CNN. Simulation results show that the overall PSR of the approach reach as high as 96% when the SNR is −6 dB.

The remainder of this paper is organized as follows. Section II introduces the recognition system framework. In Section III, the data processing algorithm is introduced in detail. And Section IV introduces the convolution neural network in detail. Section V shows the simulation results. Finally, Section VI provides conclusions.

II. SYSTEM FRAMEWORK

The received radar signal is composed of a modulated signal and noise. Its model can be written as

$$s(t) = x(t) + n(t) \tag{1}$$

where $s(t)$ and $x(t)$ are received signal and modulated signal, respectively. $n(t)$ is random noise, which is generally assumed to be additive white Gaussian noise.

The modulated signal $x(t)$ is given by

$$x(t) = Arect\left(t/T\right) e^{-j(2\pi f_c t+\phi(t)+\phi_0)} \tag{2}$$

where A is the amplitude and T is the pulse width. f_c and ϕ_0 are the carrier frequency and the initial phase, respectively. $\phi(t)$ is the phase function, which determines the modulation type of radar signal. Thus, we pay more attention to the characteristics of the phase function of the modulation signal.

In this paper, we propose a radar signal intra-pulse modulation recognition approach based on convolutional neural network. The framework of the proposed approach is shown in Figure 1. The most essential difference among the signals of different modulation types is the form of the phase function. That is, the difference in the form of the instantaneous frequency function. The core idea of the proposed approach is to transform the recognition problem of the signal modulation to the TFI recognition. From Figure 1, we can see that the approach is divided into two parts: one is the extraction and processing of the TFIs of radar signals, and the other is the recognition of the TFIs of radar signals. The extraction of the TFIs is vital for the approach. This approach requires that the extracted TFI of siganl can reflect the instantaneous frequency of the signal while having good anti-noise performance. Hence, in order to improve the quality of the TFIs, the CTFD with a new kernel function is proposed to extract

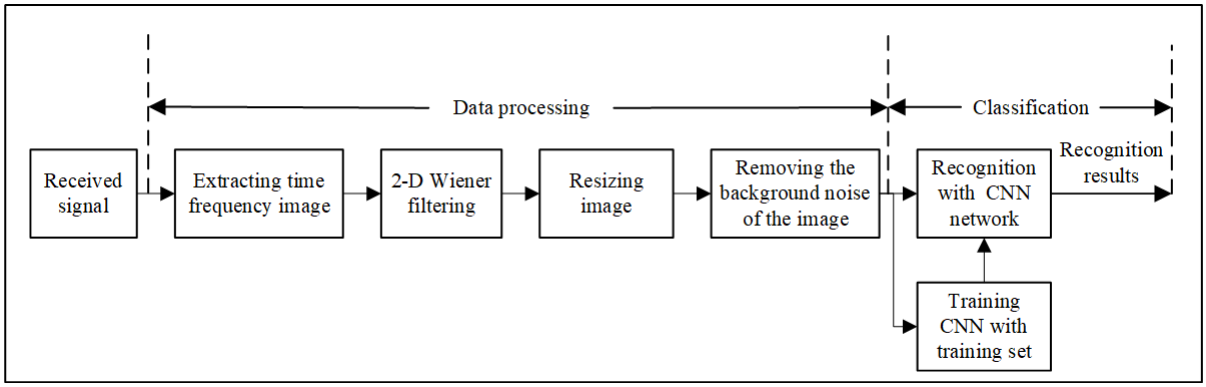

FIGURE 1. The framework of the intra-pulse modulation recognition approach proposed in this paper.

the TFIs of radar signals. For the intra-pulse modulation recognition of radar signals, we pay more attention to the morphological features of the TFIs of radar signals. In order to reduce computational complexity, the TFIs of radar signals need to be transformed into binary images. In low SNR environment, however, the extracted TFI yet exists a lot of noise that make the image binarization more difficult. Thus, 2-D Wiener filtering is used to smooth the TFI and reduce noise. After that, in order to reduce the structural complexity of the CNN, the bilinear interpolation is used to resize the TFI. The TFI is transformed into a binary image by deploying Otsu method and the background noise of the TFI of the signal is also removed. This ensures the quality of the TFI of signal and further reduces the computational burden of CNN. Finally, a CNN is designed to identify the above processed image. Radar signal intra-pulse modulation recognition is eventually accomplished.

III. DATA PROCESSING

In this section, the various methods used to process the data of the received radar signal in this paper are explained in detail, which include CTFD, Wiener filtering, bilinear interpolation used to resize image and Otsu method used to remove the background noise of the image.

A. COHEN CLASS TIME FREQUENCY DISTRIBUTION FOR TFI EXTRACTION

The most widely used methods to extract the TFI, include Short-Time Fourier Transform (STFT), Wigner-Ville distribution (WVD) and so on [23]. When using STFT to extract TFI, we need to choose the window function and its length, which can not be changed once selected. This makes the STFT lack of adaptability. Hence, the STFT is not suitable for extracting TFIs of unknown signals. As for WVD, it has very high time-frequency resolution, but its anti-noise ability is poor. For the modulated signals such as nonlinear frequency modulation signal, PSK and FSK, there will be the cross-terms that seriously affect the recognition of the modulation types of the signal. For example, for FSK signals, the cross-terms can cause false frequency-hopping, which makes it impossible to identify the FSK type based on frequency hopping. For PSK signals, there are small frequency hopping amplitude. The cross-terms can cause small frequency hopping features to be unclear, affecting the identification of PSK signals. Also, the cross-terms of modulated signal are easily affected by noise and have instability. Consequently, it is not reliable to use the cross-terms to identify signals. In short, when using TFI to identify signal, we hope to minimize the cross-terms of signal while retaining the modulation feature of signal. Cohen class time frequency distribution is able to obtain the expected properties like higher resolution, non-negative and removal of cross-terms by smoothing the WVD through time and frequency shifting with a kernel function [24]. Cohen class time frequency distribution is defined as

$$C(t,\omega) = \frac{1}{4\pi^2}\iint AF(\tau,\nu)\phi(\tau,\nu)\,\mathrm{e}^{-j\nu t - j\omega\tau}\,d\nu d\tau \tag{3}$$

$$AF(\tau,\nu) = \int x\left(u+\frac{\tau}{2}\right)x^*\left(u-\frac{\tau}{2}\right)\mathrm{e}^{j\nu u}du \tag{4}$$

where $x(u)$ is the received signal. $AF(\tau,\nu)$ is the ambiguity function. τ and ν are the time delay and the frequency shift, respectively. $\phi(\tau,\nu)$ is a kernel function. Equation (3) shows that the Cohen class time frequency distribution is a two-dimensional Fourier transform of the signal that is a signal after filtering the ambiguity function with a kernel function.

By designing the kernel function, the cross-terms of the signal can be eliminated and the noise can be reduced. Reference [25] points out that the kernel function should be a 2-D low pass filter function. The most common kernel function is a Gaussian function, $\phi(\tau,\nu) = \exp\left[-\frac{(\tau\nu)^2}{\sigma}\right]$, called CWD. The CWD can suppress cross-terms of signals and reduce noise. However, from the expression of the CWD kernel function, we can see that when $\tau = 0$ or $\nu = 0$, $\phi(\tau,\nu) = 1$. This shows that the CWD kernel function has no filtering effect on the τ axis and the ν axis. However, for radar signals, the auto-terms of the modulated signal concentrate along and around the ambiguity domain τ axis, and the maximum appears around the origin, whereas the cross-terms

exist far from the τ axis. Also, there is no auto-terms of the modulated signal on the ν axis, except at the origin. This means that for the intra-pulse modulation recognition of radar signals, the kernel function of CWD is not the best choice. Therefore, based on this characteristic of radar modulated signals, we design a new kernel function for CTFD that can extract the TFI of radar signal with better quality than CWD. This new kernel function is designed as

$$\phi(\tau, \nu) = \mathrm{e}^{-(\alpha\tau^2+\beta\nu^2)} \tag{5}$$

where α and β are two parameters that can adjust the shape of the kernel function. The width of the kernel function is estimated by 4 times of the standard difference of Gaussian function, then the width of the τ axis and the ν axis are $\sqrt{\frac{8}{\alpha}}$ and $\sqrt{\frac{8}{\beta}}$, respectively.

We give a contour map of the kernel function shown in (5) in Figure 2. As is shown in Figure 2, by adjusting the coefficients α and β, we make this kernel function distribute along the τ axis and have an elliptical shape, which fits well with the distribution of radar signals in the ambiguity domain. In Figure 3, we give the TFI of the SFM signal extracted by CWD and CTFD with a new kernel function when the SNR is -6 dB. It can be clearly seen that the quality of the TFI of the SFM signal extracted by the CTFD with a new kernel function is better than that of the CWD. This is because the new kernel function can effectively filter the ν axis compared with the kernel function of CWD, and its shape can well match the distribution characteristics of radar signals in the ambiguity domain. This makes CTFD with a new kernel function have better anti-noise ability than CWD.

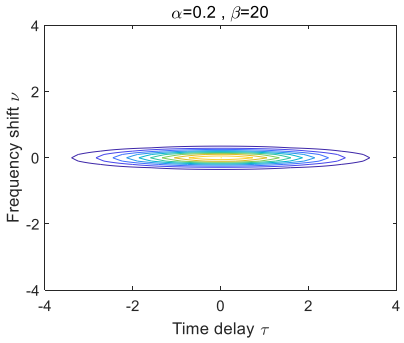

FIGURE 2. In this picture, the contour map of the kernel function designed by this paper is displayed.

In the actual signal processing, the signal is discrete, so the CTFD in this paper needs to be discretized. The following equation (6) is obtained from equation (3), (4) and (5).

$$CTFD(t, \omega) = \iint \frac{1}{\sqrt{4\pi\beta}} \mathrm{e}^{-\frac{(u-t)^2}{4\beta}-\alpha\tau^2} x\left(u+\frac{\tau}{2}\right) x^*\left(u-\frac{\tau}{2}\right) \mathrm{e}^{-j\omega\tau} du d\tau \tag{6}$$

The equation (6) is discretized as follows:

$$CTFD(n, k) = 2\sum_m \sum_l \frac{1}{\sqrt{4\pi\beta}} \mathrm{e}^{-\frac{T_s^2(l-n)^2}{4\beta}-4\alpha T_s^2 m^2} x(l+m)\, x^*(l-m)\, \mathrm{e}^{-j\frac{4\pi km}{N}} \tag{7}$$

where N is the length of the received signal, and T_s is the sampling period of signal. In this paper, we set $N = 1024$, $T_s = 1$, $\alpha = 0.0005$, $\beta = 0.001$. Figure 3 shows the TFIs of twelve different signal modulation types obtained by the CTFD.

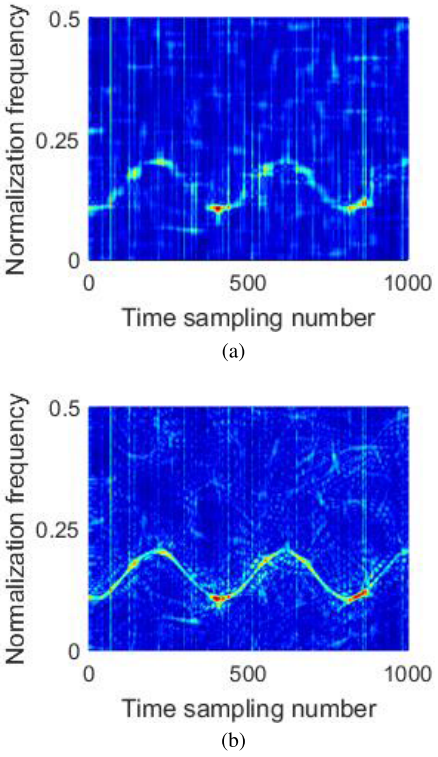

FIGURE 3. The TFI of the SFM signal extracted by CWD and CTFD with a new kernel function when the SNR is -6 dB. (a) CWD. (b) CTFD.

B. 2-D WIENER FILTERING

Though designing kernel function of CTFD can reduce noise, there still exist a lot of noise in TFI at low SNR. These noises will seriously affect the recognition of signal modulation. Therefore, we need to filter the TFI of the signal to further reduce the nosie. A Gaussian white noise stationary random process after time-frequency transform is a white noise stationary random process [21]. 2-D Wiener filtering is an adaptive filter which adjusts the effect of the filter according to the local variance of the image. It has a better filtering effect on white noise. A 2-D Wiener filtering is used to filter the TFI of the signal in this paper. We give a detailed calculation procedure for 2-D Wiener filtering. For more principles, please refer to [26].

Suppose a $m \times n$ pixel two-dimensional image is expressed in matrix $H_{m\times n}$ and each pixel can be expressed as $H(i, j)$, $i = 1, \cdots, m$, $j = 1, \cdots, n$. We need to select a filter

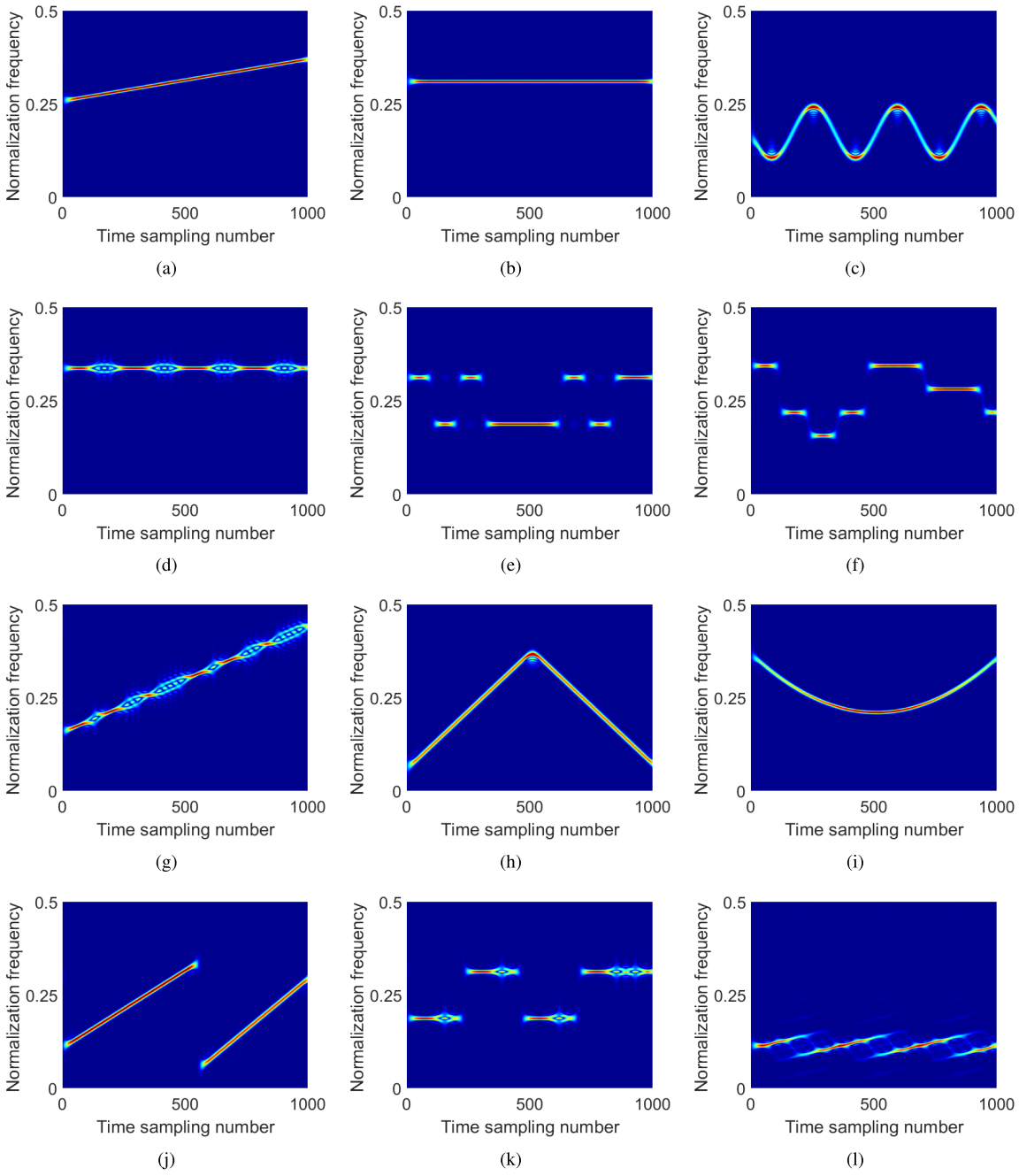

FIGURE 4. The TFIs of different modulation types signals: (a) LFM, (b) MP, (c) SFM, (d) BPSK, (e) 2FSK, (f) 4FSK, (g) LFM-BPSK, (h) DLFM, (i) EQFM, (j) MLFM, (k) 2FSK-BPSK, (l) Frank code.

neighborhood $\eta_{a\times b}$ with a pixel size of $a \times b$. Then the mean μ and variance σ^2 of the neighborhood of each pixel is calculated by equation (8) and (9).

$$\mu = \frac{1}{ab} \sum_{i,j\in\eta} H(i,j) \tag{8}$$

$$\sigma^2 = \frac{1}{ab} \sum_{i,j\in\eta} H^2(i,j) - \mu^2 \tag{9}$$

$$P(i,j) = \mu + \frac{\sigma^2 + \sigma_N^2}{\sigma^2} [H(i,j) - \mu] \tag{10}$$

Finally, the filtered image $P_{m\times n}$ can be calculated by (10). Where σ_N^2 is the noise variance, since the variance of the noise is unknown, we can replace it with the average of all the local estimates of variance. Regarding the size of $\eta_{a\times b}$, we can choose the appropriate size based on experience. Here we set $\eta_{a\times b}$ to 40×40.

C. IMAGE RESIZING AND IMAGE BINARIZATION

In order to reduce the computational complexity and simplify the complexity of the convolutional neural network classifier, we need to resize the TFI of the filtered signal. This paper uses

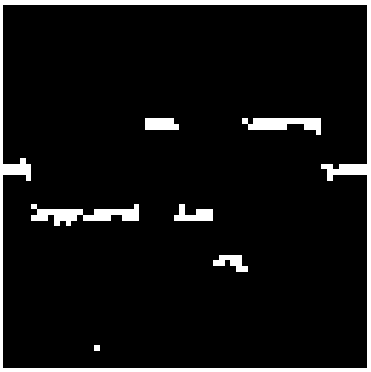

FIGURE 5. The binary image after the image in Figure 4 (b) is resized to 64×64 and binarization.

bilinear interpolation to resize the TFI. The original image $P_{m\times n}$ is resized to be the image $A_{l\times k}$ by bilinear interpolation. Then the pixel value of $A_{l\times k}$ can be calculated by equation (11) and (12).

$$A(x,y) = P(i+p, j+q) \tag{11}$$

$$\begin{aligned} P(i+p,j+q) = {} & (1+p)(1-q)P(i,j) \\ & + (1-p)qP(i,j+1) \\ & + p(1-q)P(i+1,j) \\ & + pqP(i+1,j+1) \end{aligned} \tag{12}$$

where i and p are integral parts and decimal parts of mx/l, respectively. j and q are integral parts and decimal parts of ny/k, respectively.

For the approach proposed in this paper, the morphological characteristics of the TFI of signal are crucial. In order to reduce noise and computational complexity while preserving the morphological characteristics of the image, the TFI needs to become binary image. The Otsu method is utilized to make the image binary processing in this paper [27]. The Otsu method can be written as

$$\max_{th} f(th) = \frac{N_1 N_2}{(lk)^2}\left[\frac{1}{N_1}\sum_{n=1}^{N_1} A_1(n) - \frac{1}{N_2}\sum_{m=1}^{N_2} A_2(m)\right]^2 \tag{13}$$

$$\begin{aligned} s.t.\ if\ A(i,j) \geq th, \quad & A_1 = A(i,j) \\ otherwise\ & A_2 = A(i,j) \end{aligned} \tag{14}$$

where th is the threshold, N_1 and N_2 are the length of A_1 and A_2,respectively. $A(i,j)$ needs to be converted to gray value, $A(i,j) \in [0, 255]$.

Using ergodic method to solve equation (13) and equation (14), we get the optimal threshold Th. The binary image K is given by

$$K(i,j) = \begin{cases} 1 & H(i,j) \geq Th \\ 0 & H(i,j) < Th \end{cases} \tag{15}$$

Figure 5 shows the binary image after the image in Figure 4 (b) is resized to 64×64 and binarization. As shown in Figure 5, the binary image still can well reflect the morphological features of the TFI.

IV. CLASSIFICATION

This section introduces in detail CNN and the radar signal modulation recognition approach proposed in this paper. It focuses on the basic principles of CNN and the structure of the CNN used in this paper. Then the specific steps of the proposed approach are described in detail.

A. DESIGN OF CONVOLUTIONAL NEURAL NETWORK

CNN is a kind of neural network that is specially used to process data with similar grid structure. It has excellent performance in the field of image recognition. CNN generally include convolutional layer, pooling layer, fully connected layer and activation function [28]. Figure 6 shows the CNN structure designed for classification in this paper. The CNN has a total of eight layers, including four convolutional layers, three pooling layers and one fully connected layers. The size of the input layer is 64×64×1 pixels. There are 12 neurons in the output layer, representing 12 categories. The size of the convolutional kernel is 5×5. All the other parameters have been shown in Figure 6. The following will detail the CNN calculation process.

Assume that the input size of the convolutional layer is $M \times M \times D$, denoted by I, where D is the number of channels. The size of the convolution kernel K is $N \times N \times D$ and its number is P. The stride of convolution is 1. The convolution process can be denoted as

$$\begin{aligned} S(i,j,p) = \sum_{k=1}^{D}\sum_{m=0}^{N-1}\sum_{n=0}^{N-1} & I(i+m, j+n, k) \\ & \times K_p(m,n,k) + bias_p \end{aligned} \tag{16}$$

where K_p and $bias_p$ denote the p-th convolutional kernel and its bias, respectively. S denotes convolution output and $i, j \in [1, L]$, $L = \left\lfloor \frac{M-N}{stride} + 1 \right\rfloor$.

In general, in order to obtain a nonlinear representation, a nonlinear activation function needs to be added after the convolution output. The ReLU function is a commonly used activation function in modern convolutional neural networks because it effectively suppresses the disappearance of gradients. The ReLU function is denoted as

$$f(x) = \max(0, x) \tag{17}$$

Thus, the output of the convolutional layer, called feature map, can be expressed as

$$S_{out}(i,j,p) = \max[0, S(i,j,p)] \tag{18}$$

In order to reduce data dimensions and parameters, to prevent overfitting, the pooling layer needs to be used to process the output of the convolutional layer. In this paper, we use 2 × 2 maximum pooling and its stride is 2. Therefore, the output of the pooling layer S_d is

$$S_d(i,j,p) = \max_{m,n\in\{0,1\}} \{S_{out}(2i+m-1, 2j+n-1, p)\} \tag{19}$$

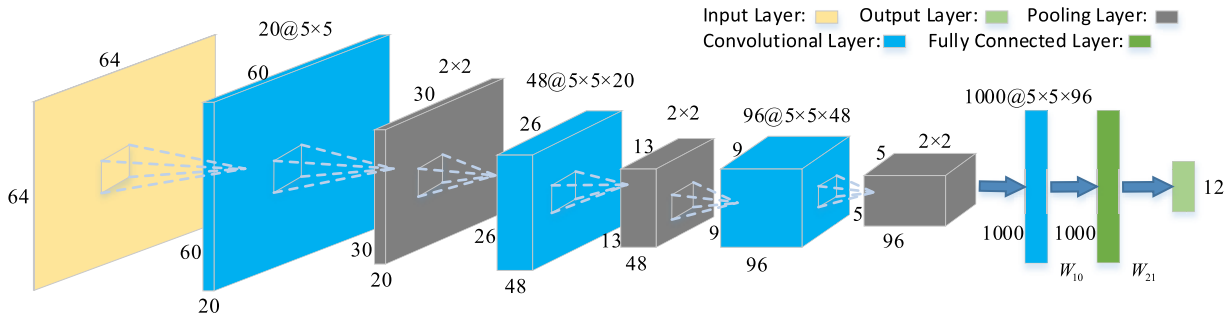

FIGURE 6. The structure of CNN designed for classification in this paper.

where $i, j \in \left[1, \left\lceil \frac{L}{2} \right\rceil\right]$. If the dimension of S_{out} is not enough, padding zero can make the dimension of S_{out} meet the requirements.

Use (16), (18) and (19) to calculate CNN until the last convolution layer. S_{last} denotes the output of the last convolutional layer. As shown in Figure 6, S_{last} is a 1000 dimensional vector. Note that W_{10} is the weight matrix of the fully connected layer and the last convolutional layer, W_{21} is the weight matrix of the output layer and the full connected layer. Thus, the calculation of the last two layers is

$$h = f\left(W_{10} S_{last} + b_1\right) \tag{20}$$

$$out = W_{21} h + b_2 \tag{21}$$

where h and out are the output of the fully connected layer and the output of the output layer, respectively. b_1 and b_2 are biases.

In order to get the probability classification result, we add Softmax function to the output layer to get the final probability classification output. The final probability classification output $\hat{y}$ is

$$\hat{y}^i = P\left(y = i | out\right) = \frac{e^{out^i}}{\sum_{i=1}^{12} e^{out^i}} \tag{22}$$

where $\hat{y} = \left[\hat{y}^1, \hat{y}^2, \cdots, \hat{y}^i, \cdots, \hat{y}^{12}\right]^T$. $\hat{y}^i$ represents the probability that the input is classified as class i. out^i represents the i-th component of the vector out. The category corresponding to the maximum $\hat{y}$ is the CNN classification result.

With regard to the optimization of CNN in Figure 6, we choose the cross-entropy as the loss function. Well, the training of the CNN can be written as

$$\min\left\{-\left[y \log\left(\hat{y}\right) + (1 - y) \log\left(1 - \hat{y}\right)\right]\right\} \tag{23}$$

where y is the one-hot encoding of the data label.

Using a stochastic gradient descent method, we can easily optimize the solution (23). In the structure of the CNN shown in Figure 6, as the depth of the convolution deepens, the height and width of the feature map decrease. In order to reduce the loss of information, deep learning research shows empirically that the depth of the feature map must increase. This means that the deeper convolutional layer has more convolutional kernels and more calculations. We follow this empirical criterion when designing the CNN. In fact, it is difficult to find the optimal hyperparameter of a CNN, but it is easy to find a set of hyperparameter that make CNN works well. According to our experiment, we set a set of hyperparameters that make the designed CNN have good classification performance. This set of hyperparameters is marked in Figure 6.

B. DETAILED PROCESS OF THE APPROACH

The basic principles of the radar signal intra-pulse modulation recognition approach based on deep convolutional neural network have been described above. The detailed process of the algorithm will be given below.

Step 1: By using equation (7), the TFI of the received radar signal is obtained as $H_{m\times n}$. In this paper, the size of the TFI is 1024×1024.

Step 2: Matrix $H_{m\times n}$ is processed by 2-D Wiener filtering, and matrix $P_{m\times n}$ is obtained. The neighborhood $\eta_{a\times b}$ size of 2-d Wiener filtering is 40×40.

Step 3: Using bilinear interpolation to resize $P_{m\times n}$ to 64×64, then using the Otsu method to obtain a matrix $K_{m\times n}$.

Step 4: The training set of CNN is obtained through the above steps, and the training set is used to train the CNN designed in this paper.

Step 5: Using the trained CNN to identify the data processed in Step 1-3, the recognition of the intra-pulse modulation of the radar signal is achieved.

V. SIMULATION RESULTS AND ANALYSIS

In this section, the performance of the proposed approach is analyzed using simulation data. The noise of signal is additive Gaussian white noise. Classification performance is measured as a function of the SNR. The SNR is defined as $SNR = 10\log_{10}\left(\sigma_s^2 / \sigma_n^2\right)$. σ_s^2 and σ_n^2 are signal power and noise power, respectively.

There are twelve kinds of simulation radar signals, including LFM, SFM, 2FSK, 4FSK, DLFM, EQFM, MLFM, BPSK, Frank, MP, LFM-BPSK and 2FSK-BPSK. The frequency parameters of the signals are normalized. In order to analyze the generalization performance of the approach, the parameters of all the simulation signals have

TABLE 1. Simulation radar signal parameter table.

Signal type	Parameter	Ranges
LFM	Initial frequency f_c	0.01∼0.45
	Bandwidth Δf	0.05∼0.4
SFM	Minimum frequency $f_{\min}$	0.05∼0.15
	Δf	0.05∼0.35
2FSK	carrier frequency f_1,f_2	0.1∼0.4
	Δf	(1/32∼1/8)$*N$
4FSK	$f_1 \sim f_4$	0.1∼0.4
	T_s	(1/32∼1/8)$*N$
EQFM	f_{min}	0.01∼0.4
	Δf	0.05∼0.3
DLFM	f_c	0.01∼0.4
	Δf	0.05∼0.35
MP	carrier frequency f_0	0.1∼0.4
MLFM	f_0	0.05∼0.15
	Δf	0.1∼0.35
	Segment length L	(0.3 0.7)$*N$
BPSK	Barker codes	[5,7,9,13]
	f_0	0.1∼0.4
	T_s	(1/32∼1/16)$*N$
Frank	f_0	0.1∼0.4
	T_s	(1/100 1/32)$*N$
	Phase number M	[4,5,6,7]
LFM-BPSK	Barker codes	[5,7,9,13]
	f_0	0.01∼0.45
	Δf	0.05∼0.4
	T_s	(1/32∼1/16)$*N$
2FSK-BPSK	Barker codes	[3,5,7]
	f_1,f_2	0.1∼0.4
	T_s	(1/16∼1/4)$*N$

where N is the length of the signal

a dynamic range. The detailed parameters of the signals are shown in Table 1. The signal length is $N = 1024$. For each kind of radar signal, we simulate 200 samples every 2 dB as training set when SNR ranges from -6 dB to 10 dB. There is a total of 21600 samples in the training set. When SNR ranges from -10 dB to 10 dB, we simulate 100 samples every 2 dB for each kind of radar signal as test set. There is a total of 13200 samples in the test set.

A. THE PSR OF THE PROPOSED APPROACH

Figure 7 shows the relation curve between the PSR and the SNR. From Figure 7, the PSR of the proposed approach is positively related to the SNR. When the SNR$\geq$0 dB, the PSR of the approach for twelve kinds of signals is 100%. When the SNR≥ -6 dB, the PSR of the approach is more than 91%. With the further decline of SNR, the PSR of the approach begins to decline clearly, especially for LFM, MP, BPSK, DLFM, EQFM and Frank signals. But when the SNR is -8 dB, the approach still maintains more than a PSR of 80% for SFM, 4FSK, LFM-BPSK, MLFM and 2FSK-BPSK. This shows that the proposed approach is effective and robust.

In order to further analyze the performance of the proposed approach, we compare the approach with the existing approach (based on [22]). In [22], the TFI of the radar signal is extracted by CWD, and then the TFI is resized and binarized using the nearest neighbor interpolation method and the global threshold method. Finally, using LeNet-5 to realize signal recognition. From Figure 7, it can be clearly seen that the PSR of the proposed approach is higher than

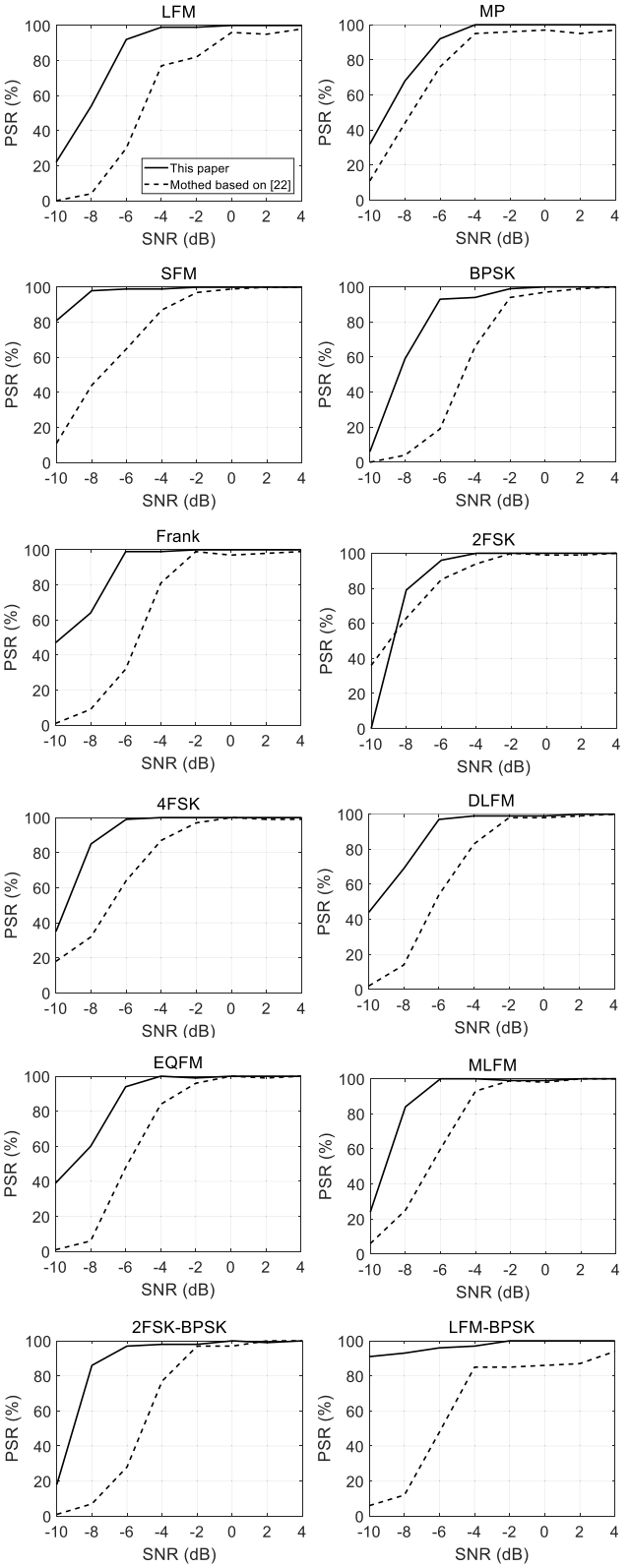

FIGURE 7. The relation curve between the PSR of signal and the SNR.

that of the existing approach for twelve kinds of signals at the same SNR. When the SNR is -6 dB, the PSR of the existing approach is very low, and the existing approach cannot

TABLE 2. Confusion matrix for the proposed approach at SNR of −6 dB.

	LFM	MP	SFM	BPSK	Frank	2FSK	4FSK	DLFM	EQFM	MLFM	2FSK-BPSK	LFM-BPSK
LFM	91	0	0	0	0	0	0	0	0	0	0	4
MP	0	92	0	5	0	0	0	0	0	0	0	0
SFM	0	0	99	0	0	0	1	0	0	0	0	0
BPSK	0	2	0	93	0	0	0	0	0	0	2	0
Frank	0	2	0	1	99	0	0	0	0	0	0	0
2FSK	0	1	0	0	0	96	0	0	0	0	1	0
4FSK	0	0	0	0	0	0	99	0	0	0	0	0
DLFM	0	0	0	0	0	0	0	97	6	0	0	0
EQFM	0	3	0	0	0	0	0	2	94	0	0	0
MLFM	0	0	1	0	0	0	0	0	0	100	0	0
2FSK-BPSK	0	0	0	1	0	4	0	0	0	0	97	0
LFM-BPSK	9	0	0	0	1	0	0	1	0	0	0	96

achieve the recognition of twelve kinds of signals. By contrast, the overall PSR of the proposed approach is 96.1% at SNR = −6 dB. This demonstrates that the proposed approach has higher PSR and stronger anti-noise ability than the existing approach. This is mainly because we have adopted different methods from [22] to extract, process and identify the TFI of radar signals. First, we designed a new kernel function for the CTFD, which has been analyzed to be more suitable for extracting the TFI of radar signal and have stronger anti-noise performance than CWD in Section III-*A*. Second, we performed 2-D Wiener filter processing on TFI before resizing and binarizing the TFI of radar signal, which can further reduce noise and improve the quality of the TFI. Third, we built a CNN deeper than LeNet-5. It has two more convolutional layers than LeNet-5, and the size of the input layer increased from 32×32 to 64×64, which makes CNN have better classification performance than LeNet-5. In addition, regarding the impact of these three points on the proposed approach, we will perform simulation analysis later.

Table 2 shows the confusion matrix for the proposed approach at SNR of −6 dB (100 tests for each signal). It can be seen from the table that the approach has a very good PSR for all twelve kinds of signals. The signals with the lowest PSR are LFM signals with a PSR of 91%. According to the confusion matrix, the recognition error occurs mainly between the signals pairs which have similar TFIs, such as LFM and LFM-BPSK signals, 2FSK and 2FSK-BPSK signals, MP and BPSK signals. This is mainly because the TFI of the BPSK signal exists some small frequency jump, which is the main difference between BPSK signal and MP signal. These small frequency jump become blurred and even lost under the influence of noise and image resizing, leading to confusion between signals.

B. THE EFFECTS OF TFI EXTRACTION AND PROCESSING ON THE PSR OF THE PROPOSED APPROACH

In order to verify the validity of the new kernel function proposed in this paper for CTFD, we compare it with CWD. The comparison result is shown in Figure 8. It can be seen from this figure that the performance of CTFD with a new kernel function for the proposed approach is better than that

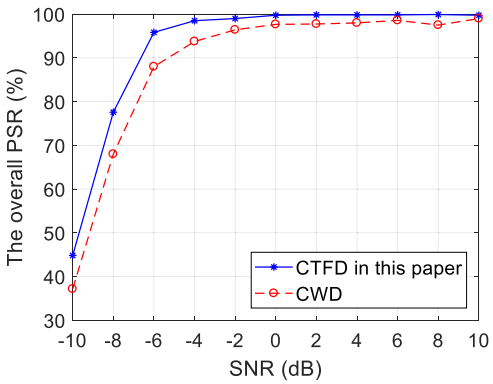

FIGURE 8. The effects of the kernel function on the PSR of the proposed approach.

of CWD. This is due to the fact that the kernel function of CWD is unable to filter the frequency shift axis in the fuzzy domain. In other words, the TFI extracted with CWD has more noise than the TFI extracted with the CTFD proposed in this paper at low SNR. Hence, the CTFD with a new kernel function has better anti-noise performance than CWD.

Figure 9 displays the TFI of the 4FSK signal before and after filtering when SNR = −4 dB. It can be clearly seen from the figure that the TFI noise of the signal is effectively smoothed after 2-D Wiener filtering. This guarantees that the binarized TFI of radar signal has less noise in a low SNR environment. Figure 10 shows the effect of 2-D Wiener filtering on this approach. As shown in Figure 10, the overall PSR of the approach without 2-D Wiener filtering is significantly lower than that of the approach using 2-D Wiener filtering at the same SNR. In particular, when the SNR = −6 dB, the approach using 2-D Wiener filtering achieved an overall PSR of 96%, while the approach without 2-D Wiener filtering had an overall PSR of only 63%. This shows that 2-D Wiener filtering can effectively improve the approach performance.

In addition, we explored the effect of the size of the CNN input layer on the performance of the approach. Figure 11 shows the effect on the overall PSR of the approach when the sizes of the CNN input layer

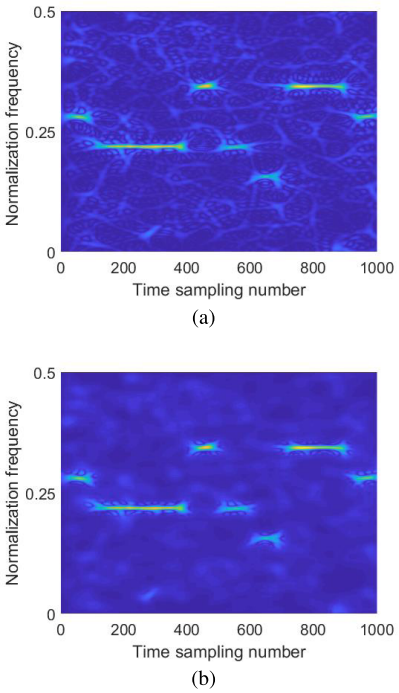

FIGURE 9. The TFI of 4FSK signal before and after 2-D Wiener filtering (SNR=−4 dB). (a) Before 2-D Wiener filtering. (b) After 2-D Wiener filtering.

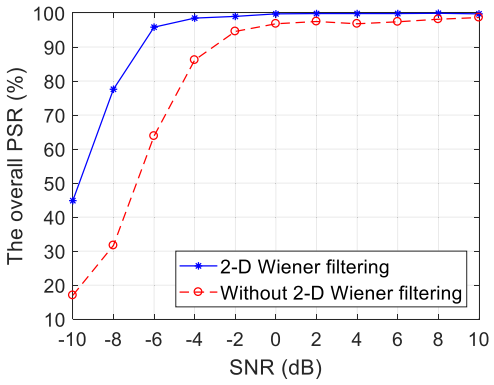

FIGURE 10. The effects of 2-D Wiener filtering on the PSR of the proposed approach.

are 32×32, 64×64 and 128×128, respectively. From Figure 11, when the CNN input layer size is 64×64, the overall PSR of the approach is highest at the same SNR (SNR≥−6 dB). There are two main reasons for the result shown in Figure 11. One reason is that if the input layer of the CNN is too small (such as 32×32), the TFI of signal will lose more detail information (such as small frequency jump of the TFI of BPSK signal), which will result in signals with similar TFI that is hard to be identified under the influence of noise. The other reason is that if the input layer of CNN is too large (such as 128×128), the number of CNN layers must be increased for the CNN model in this paper while keeping the convolution kernel size of CNN unchanged. However, an excessive number of CNN layers can lead to over-fitting

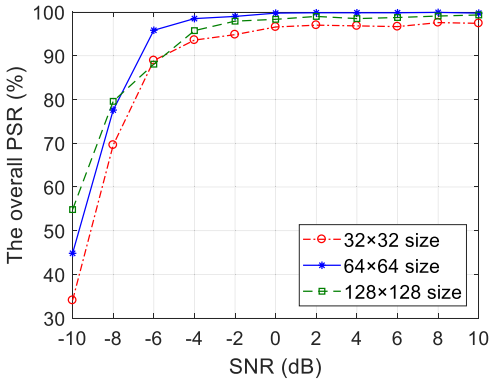

FIGURE 11. The effect of the input layer size of the CNN on the PSR of the proposed approach..

and gradient vanishing of the CNN model, thereby degrading the performance. Therefore, the size of the input layer of CNN can neither be too small nor too large. For the approach proposed in this paper, we think that it is reasonable to set the input layer size of CNN to 64 × 64.

VI. CONCLUSION

In this paper, we proposed an intra-pulse modulation recognition approach for radar signal based on convolutional neural network. The approach can identify twelve kinds of radar signals (including LFM, SFM, 2FSK, 4FSK, DLFM, EQFM, MLFM, BPSK, Frank, MP, LFM-BPSK and 2FSK-BPSK) in a low SNR environment. Simulation results show that the overall PSR of the approach is as high as 96.1% for twelve kinds of radar signals when the SNR is −6 dB. This shows that the approach is useful and reliable. The proposed approach has good adaptability and it can effectively identify radar signals with large variation range parameters. It can be used in electronic reconnaissance, electronic resistance and other fields to identify radar signals. We have only studied the modulation recognition of intra-pulse single-component radar signals in this paper. However, space electromagnetic pulse density is getting bigger and bigger. How to realize the modulation recognition of the intra-pulse multi-component radar signal has become a problem to be solved. This is also our future research work.

REFERENCES

[1] G. Latombe, E. Granger, and F. A. Dilkes, "Fast learning of grammar production probabilities in radar electronic support," *IEEE Trans. Aerosp. Electron. Syst.*, vol. 46, no. 3, pp. 1262–1289, Jul. 2010.

[2] M. Gupta, G. Hareesh, and A. K. Mahla, "Electronic warfare: Issues and challenges for emitter classification," *Defence Sci. J.*, vol. 61, no. 3, pp. 228–234, 2011.

[3] A. W. Ata'a and S. N. Abdullah, "Deinterleaving of radar signals and PRF identification algorithms," *IET Radar Sonar Navigat.*, vol. 1, no. 5, pp. 340–347, Oct. 2007.

[4] P. E. Pace, *Detecting and Classifying Low Probability of Intercept Radar*. Norwood, MA, USA: Artech House, 2004.

[5] P. Bezousek and V. Schejbal, "Radar technology in the Czech Republic," *IEEE Aerosp. Electron. Syst. Mag.*, vol. 19, no. 8, pp. 27–34, Aug. 2004.

[6] L. Zhang, N. Cui, M. Liu, and Y. Zhao, "Asynchronous filtering of discrete-time switched linear systems with average dwell time," *IEEE Trans. Circuits Syst. I, Reg. Papers*, vol. 58, no. 5, pp. 1109–1118, May 2011.
[7] W. Wei and J. M. Mendel, "Maximum-likelihood classification for digital amplitude-phase modulations," *IEEE Trans. Commun.*, vol. 48, no. 2, pp. 189–193, Feb. 2000.
[8] B. F. Beidas and C. L. Weber, "Higher-order correlation-based approach to modulation classification of digitally frequency-modulated signals," *IEEE J. Sel. Areas Commun.*, vol. 13, no. 1, pp. 89–101, Jan. 1995.
[9] T. R. Kishore and K. D. Rao, "Automatic intrapulse modulation classification of advanced LPI radar waveforms," *IEEE Trans. Aerosp. Electron. Syst.*, vol. 53, no. 2, pp. 901–914, Apr. 2017.
[10] X. Fan, T. Li, S. Su, X. Fan, T. Li, and S. Su, "Intrapulse modulation type recognition for pulse compression radar signal," *J. Appl. Remote Sens.*, vol. 11, no. 3, p. 035018, 2017.
[11] J. Dudczyk, "A method of feature selection in the aspect of specific identification of radar signals," *Bull. Polish Acad. Sci. Tech. Sci.,*, vol. 65, no. 1, pp. 113–119, Feb. 2017.
[12] Z. Yang, W. Qiu, H. Sun, and A. Nallanathan, "Robust radar emitter recognition based on the three-dimensional distribution feature and transfer learning," *Sensors*, vol. 16, no. 3, p. 289, 2016.
[13] D. Zeng, X. Zeng, H. Cheng, and B. Tang, "Automatic modulation classification of radar signals using the Rihaczek distribution and Hough transform," *IET Radar, Sonar Navigat.*, vol. 6, no. 5, pp. 322–331, Jun. 2012.
[14] J. Lunden and V. Koivunen, "Automatic radar waveform recognition," *IEEE J. Sel. Topics Signal Process.*, vol. 1, no. 1, pp. 124–136, Jun. 2007.
[15] M. Zhang, L. Liu, and M. Diao, "LPI radar waveform recognition based on time-frequency distribution," *Sensors*, vol. 16, no. 10, p. 1682, 2016.
[16] R. Girshick, "Fast R-CNN," in *Proc. IEEE Int. Conf. Comput. Vis.*, Santiago, Chile, Dec. 2015, pp. 1440–1448.
[17] H. Li, Z. Lin, X. Shen, J. Brandt, and G. Hua, "A convolutional neural network cascade for face detection," in *Proc. IEEE Conf. Comput. Vis. Pattern Recognit.*, Boston, MA, USA, Jun. 2015, pp. 5325–5334.
[18] X. Chen *et al.*, "3D object proposals for accurate object class detection," in *Proc. Int. Conf. Neural Inf. Process. Syst.*, 2015, pp. 424–432.
[19] W. Xing, Y. Zhou, D. Zhou, Z. Chen, and Y. Tian, "Research on low probability of intercept radar signal recognition using deep belief network and bispectra diagonal slice," *J. Electron. Inf. Technol.*, vol. 38, no. 11, pp. 2972–2976, 2016.
[20] D. Zhou, X. Wang, Y. Tian, and R. Wang, "A novel radar signal recognition method based on a deep restricted Boltzmann machine," *Eng. Rev.*, vol. 37, no. 2, pp. 165–172, 2017.
[21] C. Wang, J. Wang, and X. Zhang, "Automatic radar waveform recognition based on time-frequency analysis and convolutional neural network," in *Proc. IEEE Int. Conf. Acoust., Speech Signal Process.*, New Orleans, LA, USA, Mar. 2017, pp. 2437–2441.
[22] M. D. M. Zhang and L. Guo, "Convolutional neural networks for automatic cognitive radio waveform recognition," *IEEE Access*, vol. 5, pp. 11074–11082, 2017.
[23] Z. Feng, M. Liang, and F. Chu, "Recent advances in time–frequency analysis methods for machinery fault diagnosis: A review with application examples," *Mech. Syst. Signal Process.*, vol. 38, no. 1, pp. 165–205, 2013.
[24] L. Cohen, "Time-frequency distributions-a review," *Proc. IEEE*, vol. 77, no. 7, pp. 941–981, Jul. 2002.
[25] J. Jeong and W. J. Williams, "Kernel design for reduced interference distributions," *IEEE Trans. Signal Process.*, vol. 40, no. 2, pp. 402–412, Feb. 1992.
[26] J. S. Lim, *Two-Dimensional Signal and Image Processing*, vol. 34. Englewood Cliffs, NJ, USA: Prentice-Hall, 1990, pp. 6–8.
[27] N. Otsu, "A threshold selection method from gray-level histograms," *IEEE Trans. Syst., Man, Cybern.*, vol. SMC-9, no. 1, pp. 62–66, Jan. 1979.
[28] I. Goodfellow, Y. Bengio, A. Courville, and F. Bach, *Deep Learning*. Cambridge, MA, USA: MIT Press, 2016, pp. 326–366.

ZHIYU QU received the Ph.D. degree in communication and information system from Harbin Engineering University, Harbin, Heilongjiang, China, 2008. In 2008, she joined the Nanjing Research Institute of Electronic Technology, where she was studying radar signal processing and passive target tracking. She is currently an Associate Professor with Harbin Engineering University. Her current research interests include wide band signals detection, high-precision passive direction finding, and spatial spectrum estimation.

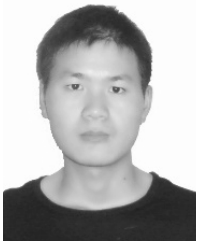

XIAOJIE MAO received the bachelor's degree from Harbin Engineering University, Harbin, Heilongjiang, China, where he is currently pursuing the master's degree. His research interests include radar signal recognition, machine learning, and image processing.

ZHIAN DENG received the bachelor's and Ph.D. degrees from the School of Electronics and Information Engineering, Harbin Institute of Technology, in 2006 and 2012, respectively. He is currently an Associate Professor with the College of Information and Communication Engineering, Harbin Engineering University, China. His current research interests include radar signal processing, wireless positioning, and machine learning.